

Evaluation of human middle ear function via an acoustic power assessment

Jont B. Allen, PhD;^{1*} Patricia S. Jeng, PhD;² Harry Levitt, PhD³

¹Department of Electrical and Computer Engineering, University of Illinois, Urbana-Champaign, IL; ²Mimosa Acoustics, Inc., Champaign, IL; ³Advanced Hearing Concepts, Bodega Bay, CA

Abstract—Measurements of middle ear (ME) acoustic power flow (power reflectance, power absorption, and transmittance) and normalized impedance (acoustic resistance, acoustic reactance, and impedance magnitude) were compared for their utility in clinical applications. Transmittance, a measure of the acoustic power absorbed by the ME, was found to have several important advantages over other measures of acoustic power flow. In addition to its simple and audiological relevant physical interpretation (absorbed power), the normal transmittance curve has a simple shape that is visually similar to the ME transfer function. The acoustic impedance measures (resistance and reactance) provided important additional information about ME status and supplemented transmittance measurements. Together these measurements can help identify unusual conditions such as eardrum perforations. While this article is largely a review of the development of a commercial power reflectance measurement system, previously unpublished experimental results are presented.

Key words: acoustic impedance, acoustic power reflectance, characteristic impedance, conductive disorders, middle ear pathologies, otitis media, otoacoustic emissions, otosclerosis, resistance, transmittance.

INTRODUCTION

The middle ear (ME) is remarkable in both its complexity and efficiency. Airborne sound that reaches the

eardrum is converted to acoustic vibration of a membrane (the eardrum). This vibration drives a mechanical lever system (the ossicles) that transmits the acoustic signal to a second membrane (the oval window) that, in turn, conveys the signal to incompressible fluid in the cochlea. Relatively little acoustic power is lost from the ear canal to the inner ear (<3 dB) in this complex sound transmission system. In addition, the system is extremely sensitive. Sounds of very low intensity are transmitted efficiently from eardrum to cochlea. The threshold of hearing at 1 kHz is near 0 dB sound pressure level (SPL), which corresponds to a motion of the stapes of around 1 pm.

Abbreviations: DPOAE = distortion product otoacoustic emission, DSP = digital signal processing, HL = hearing level, IRB = institutional review board, ME = middle ear, OME = otitis media with effusion, SPL = sound pressure level.

This material was based on work supported by the National Institute on Deafness and Other Communication Disorders (grant 1 R43 DC03138-01). The National Center for Rehabilitative Auditory Research is also gratefully acknowledged for its assistance.

*Address all correspondence to Jont B. Allen, PhD; Department of Electrical and Computer Engineering, University of Illinois, 2061 Beckman Laboratory, Urbana-Champaign, IL 61801; 217-244-9567; fax: 217-367-9741. Email: jontalle@uiuc.edu
DOI: 10.1682/JRRD.2005.04.0064

Also, relatively little power is lost for retrograde signals; i.e., signals traveling in the reverse direction from the oval window to the eardrum. As a result, low-level vibrations that are generated in the cochlea by nonlinear motions of the outer hair cells can be measured in the ear canal. The measurement of these signals, known as otoacoustic emissions, is an important tool for studying the mechanism of hearing and has led to the development of powerful new techniques for the objective assessment of hearing, such as cost-effective methods of hearing screening.

The ME is also remarkably robust. Sounds of extremely high intensity (on the order of 120 dB SPL) will not damage it. The inner ear, in contrast, is subject to substantial damage from sounds of this intensity (the cilia of the outer hair cells are easily damaged, which can result in sensorineural hearing loss). The ME provides an effective protective mechanism in the form of the acoustic reflex, which helps protect the cochlea from intense low-frequency vibration that can be transmitted to the ear by bone conduction, for example, during chewing. This mechanism also protects the inner ear from intense sound, but only to a limited extent; the acoustic reflex is too slow to protect the inner ear from intense sounds of short duration [1].

However, there is a price to be paid in that the ME is a complex mechanism with many components. Each component can fail, which means that there are many possible disorders of the ME. These disorders include fluid in the ear, ossification of the bony structures, discontinuities of the ossicular chain, and perforation of the eardrum as well as abnormalities of the membranes, ligaments, and supporting structures. Since the ME is involved in virtually every test of hearing, it is critical to ascertain the status of the ME at the outset of any audiological evaluation and, in the case of abnormal ME function, pinpoint the cause so an appropriate intervention can be established.

The rapidly growing use of otoacoustic emissions for hearing screening and related diagnostic evaluations has focused attention on the need for improved methods of ME assessment [2]. The status of the ME is of key importance for the measurement of otoacoustic emissions since the external signal that travels toward the cochlea as well as the evoked retrograde otoacoustic emissions are both subject to attenuation from abnormal ME impedance changes.

A major factor that contributes to the high cost of large-scale (e.g., universal) hearing screening programs is the high rate of false positives. This rate is high because of the inability of current screening methods to distinguish between minor conductive disorders (such as a temporary blockage in the ear canal or ME) and serious inner-ear pathologies (such as a sensorineural hearing loss). The practical consequences of this problem are severe since the incidence of conductive disorders is roughly 30 times greater than that of inner-ear pathologies in infants [3–5]. Consider, for example, a universal screening program for infants; for every 1,000 infants screened, we might expect 2 or 3 to have an inner-ear pathology (0.2%–0.3%) and 50 to 100 to have a conductive disorder (5%–10%). Virtually all the infants with a conductive disorder will fail the screening test and subsequently require a more extensive evaluation, which is expensive in both time and effort.

In addition to high false-positive rates, most hearing screening programs have a narrow scope. The primary objective of these screening programs is to identify children with inner-ear pathologies that can cause negative long-term consequences. Very few screening programs attempt to identify ME pathologies in infants and newborns because of the poor reliability of instruments designed for this purpose and the testing difficulty. A significant weakness of these screening programs exists since chronic conductive disorders, such as serous otitis media, also have serious and long-term negative consequences and need to be identified early.

In order for a hearing screening program to be cost-effective, the false-positive rate needs to be substantially reduced (e.g., reduction by a factor of 30 or more would make false-positive rates negligibly low and referral rates acceptable). An efficient way of reducing the false-positive rate would be use of a test that could distinguish between conductive disorders and inner-ear pathologies. Our approach to this problem is to measure acoustic power reflectance simultaneously with otoacoustic emissions so that we can evaluate the status of the ME. Fortunately, instrumentation developed for otoacoustic emission hearing screening can be modified for measuring acoustic power reflectance. An instrument that combines these measurements has the potential to simultaneously screen for both ME and inner-ear pathologies. This would not only reduce the false-positive rate and improve cost-effectiveness, it would also allow for the identification of a range of different pathologies. A clinical

evaluation of an instrument of this type is currently in progress [6–8].*

This article is concerned with the application of power reflectance measurements and related variables for identification of various kinds of ME pathologies. Several alternative representations of the acoustic properties of the ear (power reflectance, transmittance, and acoustic impedance) were compared for different ME pathologies. Measurements were obtained with instrumentation that was initially developed for otoacoustic emission hearing screening and that had been modified for measurement of acoustic power reflectance by a method developed by Allen [9], Voss and Allen [10], Keefe [11], and Keefe et al. [12].

Impedance Discontinuities and Reflected Acoustic Power

Consider an acoustic pressure wave that travels along the ear canal. As long as no discontinuities exist in the ear canal (e.g., abrupt change in cross-sectional area from a buildup of ear wax), the acoustic power that is conveyed by the pressure wave propagates unimpeded to the eardrum. The eardrum then efficiently and smoothly, with respect to frequency, conducts the acoustic power into the ME. Some of the incident power that reaches the eardrum enters the ME, while the remainder is reflected back into the ear canal. The reflected power takes the form of a retrograde (backward-moving) pressure wave in the ear canal. Power reflectance is defined as the percentage of incident power reflected back into the ear canal.

The term “impedance of the middle ear” is a bit of a misnomer. Impedance is measured at a microphone location. The impedance of the eardrum might be inferred if one knew the exact distance from the microphone to the eardrum. However, the possibility does not exist to know this length in any practical situation because the eardrum is at an angle (i.e., the length is not precisely defined). The

mechanical load on the eardrum is from the ME; thus, when one says “the impedance of the middle ear,” what one really means is the ear-canal impedance at the microphone location, which is a delayed version of the drum impedance that includes the impedance load of the ME.

Power reflectance varies as a function of frequency and depends on how the acoustic impedance of the eardrum varies with frequency. At frequencies below 1 kHz, the impedance of the eardrum is due mostly to the stiffness of the annular ligament [13]. When pressure waves at these low frequencies reach the stapes, almost all of their power is briefly stored as potential energy in the stretched ligament and then returned to the ear canal as a retrograde pressure wave. At even lower frequencies (<0.8 kHz), only a small proportion of the incident power is absorbed into the ME [14]. The impedance of the eardrum in this frequency region essentially consists of a stiffness-based reactance and a relatively small resistance. The stiffness-based reactance is inversely proportional to frequency (i.e., it is halved with each doubling of frequency), while the resistance varies only slightly with frequency. For frequencies at the low end of the auditory range (e.g., 0.1 kHz), the reactance is more than 10 times larger than the resistance, but in the region of 1 kHz, the reactance and resistance are of comparable magnitude.

At frequencies above 6 kHz, the mass-based reactance of the ossicles becomes increasingly important and, because it is linearly proportional to frequency, dominates eardrum impedance. To further complicate matters, our experimental knowledge of eardrum impedance is relatively poor at frequencies above 6 kHz; thus, the frequency at which mass-based reactance becomes the dominant component of eardrum impedance is unknown. When a high-frequency pressure wave reaches the eardrum and mass-based reactance is substantial, most of the power in the incident pressure wave is momentarily stored as kinetic energy, primarily in the ossicles, and then returned to the ear canal as a retrograde pressure wave. At high frequencies, much of the published data shows an impedance that approaches that of a mass as the frequency is increased. Mass-based reactance is linearly proportional to frequency (i.e., it doubles with each doubling of frequency), while cochlear resistance varies only slightly with frequency [15]. Between 1 and 5 kHz the resistance and reactance are of comparable magnitude, whereas at very high frequencies the reactance can be several times greater than the resistance.

*Hunter LL. Wideband reflectance of the middle ear: Implications for infant hearing assessment. The 5th Biennial Audiology Symposium. Innovations in Hearing. The Cleveland Clinic; 2004 Apr 6–7; Cleveland, OH.

Hunter LL, Jeng P, Jackson A, Propes S. Detection of otitis media with effusion using wideband reflectance in children. Proceedings of the 5th Extraordinary International Symposium on Recent Advances in Otitis Media: Innovations in Otitis Media; 2005 Apr 24–27; Amsterdam, the Netherlands.

Vander Werff KR, Prieve BA, Georgantas LM. Comparison of middle-ear measures and ABR air-bone gap in infants. 2004 American Auditory Society Science and Technology Meeting; 2004 Mar 7–9; Scottsdale, AZ.

In a normal ear, in the midfrequency region between 1 and 5 kHz, the stiffness- and mass-based reactances of the ME interact in a complex way and largely cancel each other. The ME is a complex structure that consists of several stiffness components and several mass components that all work in harmony such that the near cancellation of reactance occurs over a wide frequency range (1 to 5 kHz). As a result, most of the incident power that reaches the eardrum in this region is absorbed into the ME and transmitted to the inner ear. In the low- and high-frequency regions the eardrum resistance is typically small compared with its reactance, whereas in the midfrequency region the resistance is larger than the combination of the stiffness- and mass-based reactances.

It should be noted that if the characteristic impedance of the ear canal were terminated at the eardrum, there would be no reflection from the eardrum and all of the incident power would enter the ME. The specific characteristic impedance of air is a pure resistance value that is denoted ρc , where ρ is the density of air and c is the speed of sound in air. Similarly, the characteristic impedance of the ear canal ($\rho c/A$) is also a resistance value (A = estimate of the cross-sectional area of the ear canal). The resistance of the eardrum is similar in magnitude to the characteristic impedance of the ear canal ($\sim 9.0 \times 10^6$ rayls). Thus, in the midfrequency region from 1 to 5 kHz, the ear canal is terminated by resistive impedance that is close to its characteristic impedance.

However, the hearing threshold is relatively poor (high) at frequencies below 1 and above 10 kHz. These are the frequency regions where the reactance of the eardrum is substantially greater than its resistance and most of the incident acoustic power is reflected back into the ear canal. In contrast, the hearing threshold is low (good) in the frequency region between 1 and 5 kHz, which is also the frequency region in which the impedance of the eardrum is approximately equal to the characteristic impedance of the ear canal. In this midfrequency region, about 50 percent of the acoustic power that reaches the normal eardrum is efficiently transmitted into the ME.

Measurement of Acoustic Power Reflectance

The magnitude and latency of the acoustic power that is reflected by the eardrum, as a function of frequency, is a useful indicator of the status of the ME. Reflected acoustic power that is significantly different in magnitude or latency from that of the normal ear will likely reveal the precise nature of a disorder.

When measuring acoustic power reflectance, we must keep in mind the nature of the quantities that are being measured. In the frequency domain, a pressure wave is a complex quantity and is specified in terms of both amplitude and phase. In mathematical terms, a pressure wave consists of both real and imaginary components. The sum of the squares of the real and imaginary terms is proportional to the power of the plane wave.

The ratio of the forward-moving (incident) pressure wave to the reflected (retrograde) pressure wave is called the pressure reflectance $R(f)$. The square of the pressure reflectance is called the power reflectance $|R(f)|^2$ and represents the fraction of power reflected by the ear structures (both cochlear and ME). Both the pressure and power reflectances are frequently expressed as percentages rather than fractions.

The latency of the reflected power can be determined from the phase of the reflected signal (latency is proportional to the rate of phase change with frequency). Thus, a proper analysis can provide both power magnitude and latency information.

Finally, the complex acoustic impedance of the ear canal (the ME impedance is measured at the microphone location in the ear canal) can be derived from the pressure reflectance and vice versa. The real component of the complex acoustic impedance is the resistance, while the imaginary component is the reactance.

Measurement Technique

Ear-canal reflectance and impedance were robustly measured with the use of the multicavity technique developed by Allen [9–10,14]. An ear-canal probe that consists of an earphone (receiver) and microphone (transmitter) is inserted into the ear canal. The earphone generates the test sound while the microphone measures the pressure in the ear canal. The acoustic properties of the probe system are determined with the use of frequency responses in four couplers (rigid cavities) of carefully chosen lengths. These five pressures (the ear-canal pressure and the four cavity pressures) are then processed to produce an estimate of the ear-canal power and pressure reflectance. Etymotic Research, Elk Grove Village, Illinois, developed the distortion product otoacoustic emission (DPOAE) ear-canal probe used in this investigation, the ER-10C. The frequency-response measurements were obtained with the use of *SysID*, which is an automated acoustic sweep-frequency (chirp) full-duplex measurement algorithm used in the DPOAE measurement system

created by Mimoso Acoustics, Inc., (Champaign, Illinois) and was developed by one of the authors (Allen) in the early 1980s for calibrating transducers in animal experiments.

Similar methods of measuring reflectance and impedance have been developed in recent years. These techniques frequently use a multicavity approach and differ primarily in terms of the size and number of calibration cavities [11,16]. Reflectance can also be derived from measurements of acoustic impedance with other methods such as the Zwislocki impedance bridge, the two microphone method, or the standing-wave tube method [15]. These various methods for measuring the acoustic impedance of the ear have been developed over the years [17]. The Zwislocki bridge is a null technique in which an adjustable acoustic impedance in one arm of the bridge is matched to the acoustic impedance of the ear. The tester detects the null condition by listening to the difference signal. This technique is both difficult and time-consuming, with lots of “hands-on” controls, as are most other methods of directly measuring acoustic impedance; therefore, these methods are not well suited for clinical use. Many of these early methods have also proven to be relatively inaccurate. In contrast, the four-cavity method used in this study is suitable for clinical use and has been shown to be accurate from 0.1 to 6.0 kHz, as determined by measurements of standard couplers with known impedance [9] and a pair of standard acoustic resistors of known resistance [10].

Clinical instruments (tympanometric methods) have been developed for measuring the reciprocal of impedance (i.e., admittance) at a few frequencies, but the frequency range of these instruments is limited and they do not provide reliable data above 1 kHz. While these methods are still being validated, they presently do not work in young infants because of the very compliant nature of the infant ear canal (Margolis et al. [18] and Keefe and Simmons [19] for recent research on the combination of tympanometric and reflectance measurements).

The reflectance measurement protocol in this study, which includes measurements of acoustic impedance and related acoustic properties of the ear, uses technology that was initially developed for otoacoustic emission hearing screening [20]. The measurements have a bandwidth of 0.1 to 6.0 kHz, which is substantially greater than the bandwidths of most clinical instruments currently in use for assessing ME function (e.g., instruments for measuring acoustic immittance). Unlike tympanometry, the system described here does not vary the static pressure

that is applied to the eardrum. While such a measurement is useful for determining the static pressure behind the eardrum, it greatly complicates acoustic power assessment.

METHODS

Four sets of data are described for illustration and were collected in different laboratories with different power flow measurement equipment. These data are unpublished except for the infant otitis media with effusion (OME) data. The first three data sets for the adult cases (normal, otosclerosis, and perforated ear drum) were collected with the use of the Reflectance Measurement System IV (Mimoso Acoustics, Inc.), which consists of a digital signal processing (DSP) board, a preamplifier, an ER-10C probe, and a calibration cavity set (CC4-V). The OME data were collected with the Multiple Frequency Impedance and Reflectance Power Flow Analyzer system that consists of a laptop computer with a DSP board, an ER-10C probe, and a similar cavity set (CC4-II). The power flow and reflectance measurements are based upon the four-cavity eardrum acoustic impedance measurement methods developed by Allen [9].

The data for the three adult ears were collected while the subjects were sitting in a quiet office. Repeated measurements were obtained for each test ear whenever possible. The subjects included a female in her 50s for the normal case, a female in her 20s for the case of otosclerosis, and a female in her 30s for the case of the perforated eardrum. The status of each tested ear was based on a prior clinical diagnosis. DPOAE measurements were obtained from the normal and otosclerotic ears at the time of reflectance measurements. The OME data was collected from a 4-year-old child during a previous study [21]. The subjects in that study were evaluated by certified audiologists. Audiometric evaluation included air- and bone-conducted audiograms and tympanometry at 0.226, 0.678, and 1.0 kHz that was measured with the Grason-Statler, Inc., GSI-33 Middle-Ear Analyzer. All data were collected with subjects' consent or parents' consent for the minor subject under local institutional review board (IRB) guidelines. The IRB for the normal and the otosclerosis cases was the University of Illinois, Urbana-Champaign, Illinois; the perforated ear drum case was the Carle Foundation Hospital, Urbana, Illinois; and the OME case was the Albert Einstein College of Medicine, Bronx, New York.

The reflectance measurement protocol comprises two steps. The first step is to calibrate the ER-10C ear probe by measuring its Thévenin equivalent parameters, source pressure, and impedance with the same diameter ear tip as for the test ears. This requires measurement of the pressure-frequency responses of the probe for four cavities of different sizes and computation of Thévenin equivalent parameters from the four pressure-frequency responses of the probe. The second step includes measurement of pressure-frequency response from the test ear and the computation of power reflectance with the use of the Thévenin equivalent parameters of the probe. The test ear's reflectance and immittance (and other derived parameters) can be computed and plotted from these measurements. In all four cases, the probes and ear tips that were used for reflectance measurements were calibrated immediately before the measurement.

The instrumentation that was used in these investigations employs computer-generated stimuli, automated data monitoring, and advanced signal processing for noise and artifact rejection. Data can be collected rapidly and conveniently. Once the system has been calibrated, which takes less than 5 minutes and is typically performed once per day depending on the experimental environment, and the probe has been placed in the subject's ear (2–3 min), the time for measuring the wideband reflectance of an ear is less than 30 s.

RESULTS

Our hypothesis is that the power reflected from an ear with an ME impairment differs from that of a normal ear and this difference is characteristic of the nature of the ME pathology, hence, the interest in the use of wideband reflectance measurements as a clinical tool [22]. Power reflectance ($|R(f)|^2$) is only one of several possible acoustic variables that can provide useful information on the status of the ME. Other derived parameters of interest are power absorption ($1 - |R(f)|^2$), transmittance (power absorption in decibels = $10 \times \log[1 - |R(f)|^2]$), and several forms of acoustic impedance ($Z(f)$) such as the reactance, resistance, and impedance magnitude ($|Z(f)|$).

Again, it is important to bear in mind that pressure reflectance $R(f)$ and impedance $Z(f)$ are complex quantities that have both magnitude and phase and that the real component of $Z(f)$ is the resistance, while the imaginary component of $Z(f)$ is the reactance.

Clinically, it is of interest to determine which of these variables provides the most information about the status of the ME. The figures provide an illustrative comparison of the acoustic characteristics of the ME: power reflectance, power absorption, transmittance, acoustic resistance, acoustic reactance, and acoustic impedance magnitude.

In each case, the variable of interest is shown as a function of frequency (on a logarithmic axis). Under certain conditions, data can be obtained over a frequency range from 0.1 to >10 kHz. The normalized values were obtained by dividing acoustic resistance, reactance, and impedance, respectively, by the characteristic impedance of the ear canal, $\rho c/A$. Note that the resulting normalized resistance, reactance, and impedance magnitude are dimensionless since each is the ratio of two quantities with the same units. Normalized values are used to reduce between-subject and between-test variability. The normalization process takes into account between-subject differences in the physical size of the ear (an important consideration when comparing male, female, and juvenile data) as well as differences in ambient temperature and atmospheric pressure at the time of testing. Both ρ and c are temperature and pressure dependent. At normal atmospheric pressure (0.751 mHg), the characteristic impedance of the average adult male ear ($\rho c/A$) at body temperature (37 °C) is 9.01×10^6 rayls. At room temperature (22 °C), $\rho c/A = 9.24 \times 10^6$ rayls; therefore, ambient temperature has an effect on acoustic impedance [18]. This is important when comparing coupler with in-the-ear measurements of acoustic impedance. The use of normalized acoustic impedance circumvents this temperature and variable area problem.

Normal Adult Female

Figure 1 shows data for a female subject in her 50s with clinically normal hearing. The blue curve relates to the left ear, the red curve to the right ear, and the yellow curve to the control based on the standard Brüel & Kjær (B&K) (Norcross, Georgia) 4157 artificial ear coupler [10]. **Figure 1(a)** shows power reflectance. Power reflectance of the B&K 4157 coupler, which represents the average adult ear, is close to 100 percent at 0.2 kHz and decreases monotonically with increasing frequency up to 1 kHz. At 1 kHz, it is close to 40 percent, with a very shallow minimum below 40 percent at 3 kHz. Power reflectance then increases above 50 percent with increasing frequency. The data for the two ears are very similar to that of the standard coupler at frequencies up to 3 kHz. At higher frequencies, the power reflectances of the two

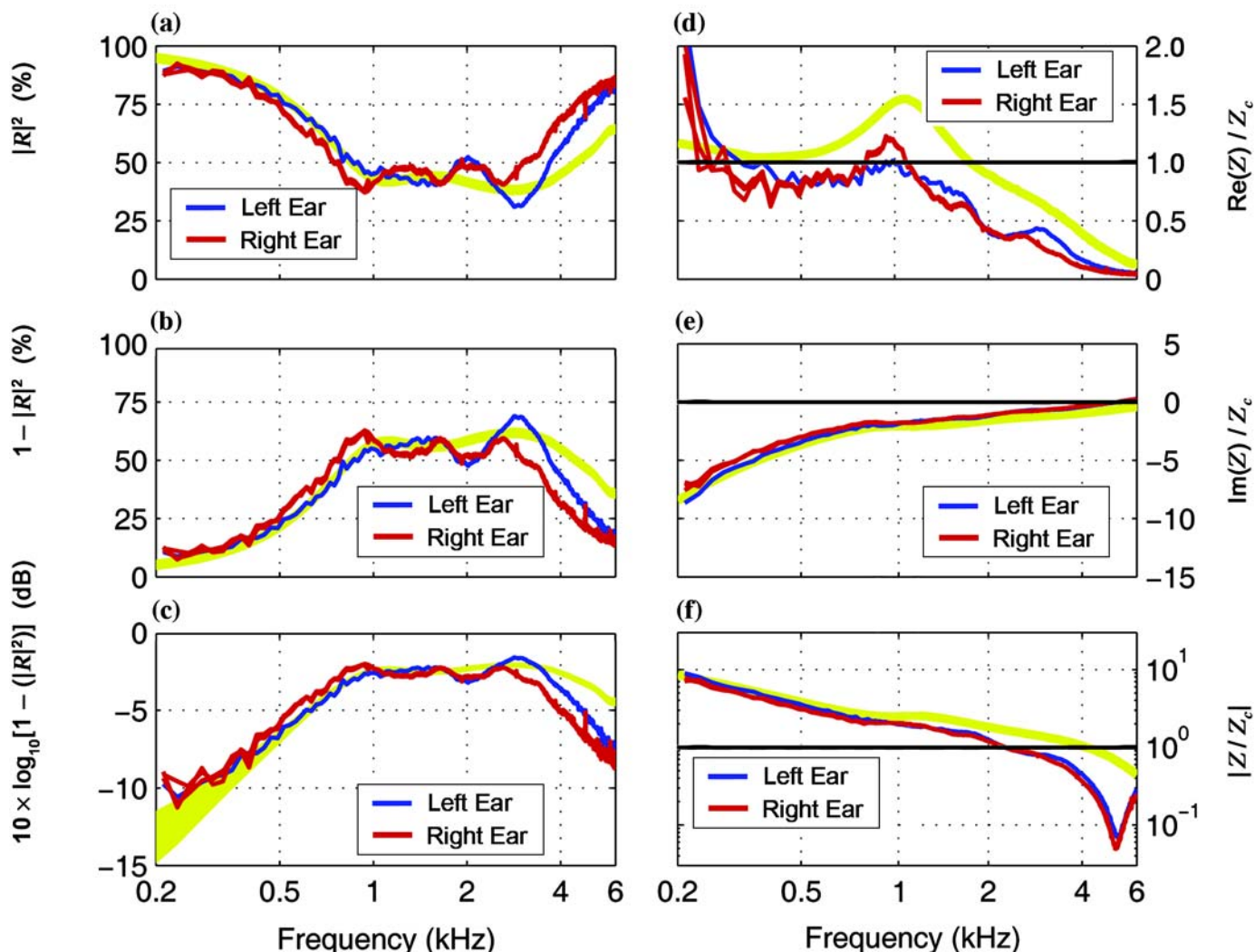


Figure 1.

Adult female with normal hearing: Six acoustic properties of middle ear shown as function of frequency on a logarithmic scale (x -axes) from both left (blue) and right (red) ears. Plots in yellow represent control (standard artificial ear coupler). (a) Power reflectance ($|R|^2$) in percent, (b) power absorption ($1 - |R|^2$) in percent, and (c) transmittance ($10 \times \log_{10}[1 - (|R|^2)]$) in decibels. (d) Normalized resistance, real (Re) component [$\text{Re}(Z)/Z_c$] (e) normalized reactance, imaginary (Im) component [$\text{Im}(Z)/Z_c$]; and (f) normalized impedance magnitude ($|Z/Z_c|$). Normalized values were obtained by dividing acoustic resistance, reactance, and impedance, respectively, by characteristic impedance of ear canal. Resulting normalized resistance, reactance, and impedance magnitude are dimensionless since each is ratio of two quantities with same units. Frequency ranges from 0.2 to 6.0 kHz.

ears differ slightly from each other and have a higher reflectance than that of the coupler.

Three repeated measurements were obtained from the right ear and one from the left ear. The equivalent volumes that were computed from the power reflectance curves are 1.56, 1.57, and 1.58 cm^3 for the right ear and 1.38 cm^3 for the left ear. All the repeated measurements are shown as multiple curves in the corresponding plots with such small variability that they appear as one curve.

The power absorption data (**Figure 1(b)**) mirror this result. Power absorption for the coupler as well as for the two ears is about 5 percent at 0.2 kHz and increases with frequency until it is relatively flat at 1 kHz. It then reaches a shallow peak at 3 kHz. The average power absorption in this peak region is close to 60 percent. The power absorption for the standard coupler decreases with frequency above 3 kHz and falls below 50 percent at frequencies above 4.5 kHz. The data for the two ears follow

a similar pattern above 3 kHz but with a greater decrease in power absorption with increasing frequency than the standard coupler.

The physical interpretation of these data is that at frequencies below 1 kHz, there is an increasing impedance mismatch at the entrance to the ME and that most of the acoustic power that reaches the eardrum at these frequencies is reflected back into the ear canal. In contrast, the ME absorbs most of the acoustic power in the frequency region between 1 and 5 kHz. This also happens to be the frequency region in which the ear is most sensitive to sound. Because the measurements were made with the use of insert earphones, the free-field pinna response is absent from these measured responses.

Figure 1(c) shows the transmittance, which is the absorbed power transformed to a logarithmic (decibel) scale. Transmittance increases linearly with frequency in the low-frequency region below 1 kHz and decreases slightly with frequency in the region above 4 kHz. The low-frequency (<1 kHz) slope is approximately 6 dB per octave (20 dB per decade), which corresponds to the impedance of a simple compliance.

This figure not only clearly illustrates the absorption of acoustic power by the ME, it also displays a relatively simple picture, in terms of straight-line approximations, of normal power absorption as a function of frequency. In addition, the use of a decibel scale allows for direct comparisons with other relevant data, such as audibility threshold in decibel SPL.

Figure 1(d) shows the normalized acoustic resistance (the real component of acoustic impedance) of the ear canal. The normalized resistance for the coupler is a little over 1.0 in the low frequencies, rises to 1.6 at 1 kHz, and decreases with frequency to ~0.2 at 6 kHz. The data for the two ears show a similar pattern except that the normalized resistance at 0.2 kHz is on the order of 2 and then falls rapidly with frequency to a value just below 1.0 and remains at this value until 1 kHz, after which it steadily declines with increasing frequency. The between-ear differences are relatively small. The normalized resistance for the two ears is close to 1.0 over a fairly wide frequency range; for this pair of ears the resistance of the eardrum is roughly equal to the characteristic impedance of the ear canal ($\rho c/A \approx 9.0 \times 10^6$ rayls) over this frequency range.

As shown in the normalized reactance data (**Figure 1(e)**), the reactance of these two ears is not negligible in the midfrequency region; this means that the

impedance of the eardrum is not entirely resistive and provides only a moderately good match to the characteristic impedance of the ear canal. As a result, about 50 percent of the incident power is reflected back into the ear canal. In terms of transmittance, this corresponds to a loss of 2 to 3 dB in the frequency region from 1 to 4 kHz. It should be noted that the reactance of the two ears and that of the standard coupler are in excellent agreement over the entire frequency range.

Over most of the midfrequency range, the magnitude of the reactance (**Figure 1(e)**) is larger than that of the resistance (**Figure 1(d)**), which is approximately equal to the characteristic impedance of the ear canal; this results in relatively efficient power transmission to the ME. Above 3 kHz, the magnitude of the reactance changes from a stiffness- to a mass-based reactance at which point the power transmission to the ME becomes relatively poor because of the mismatched resistance.

The normalized impedance magnitude is shown in **Figure 1(f)**. This is a concise way of representing impedance in that it summarizes the overall magnitude of the impedance without regard to whether stiffness-based reactance, mass-based reactance, or resistance is the dominant component. Logarithmic scales are used for both the ordinate and abscissa, and the expectation is that in the frequency regions where reactance is the dominant component, the impedance magnitude varies linearly with frequency. In the low frequencies, impedance magnitude is inversely proportional to frequency because the dominant component, a stiffness-based reactance, is inversely proportional to frequency. At 5 kHz the reactance goes to zero where the impedance magnitude has a local minimum and is equal to the ear-canal resistance.

Bilateral Otosclerosis

Figure 2(a)–(f) shows data for a female adult in her 20s with bilateral otosclerosis. Three repeated measurements were obtained for the right ear and five for the left. All the repeated measurements were plotted as shown by the multiple curves. The means of each ear are shown as black dashed lines. The equivalent volumes were computed for the right ear based on a linear regression of the reactance at low frequencies as 0.8, 0.8, and 0.87 cm³ and for the left ear as 0.93, 0.95, 0.95, 1.06, and 0.98 cm³. These numbers are typical of the equivalent volume test-retest variability.

The reflectance data (**Figure 2(a)**) show that below 0.8 kHz, most of the acoustic power that reaches the ME is

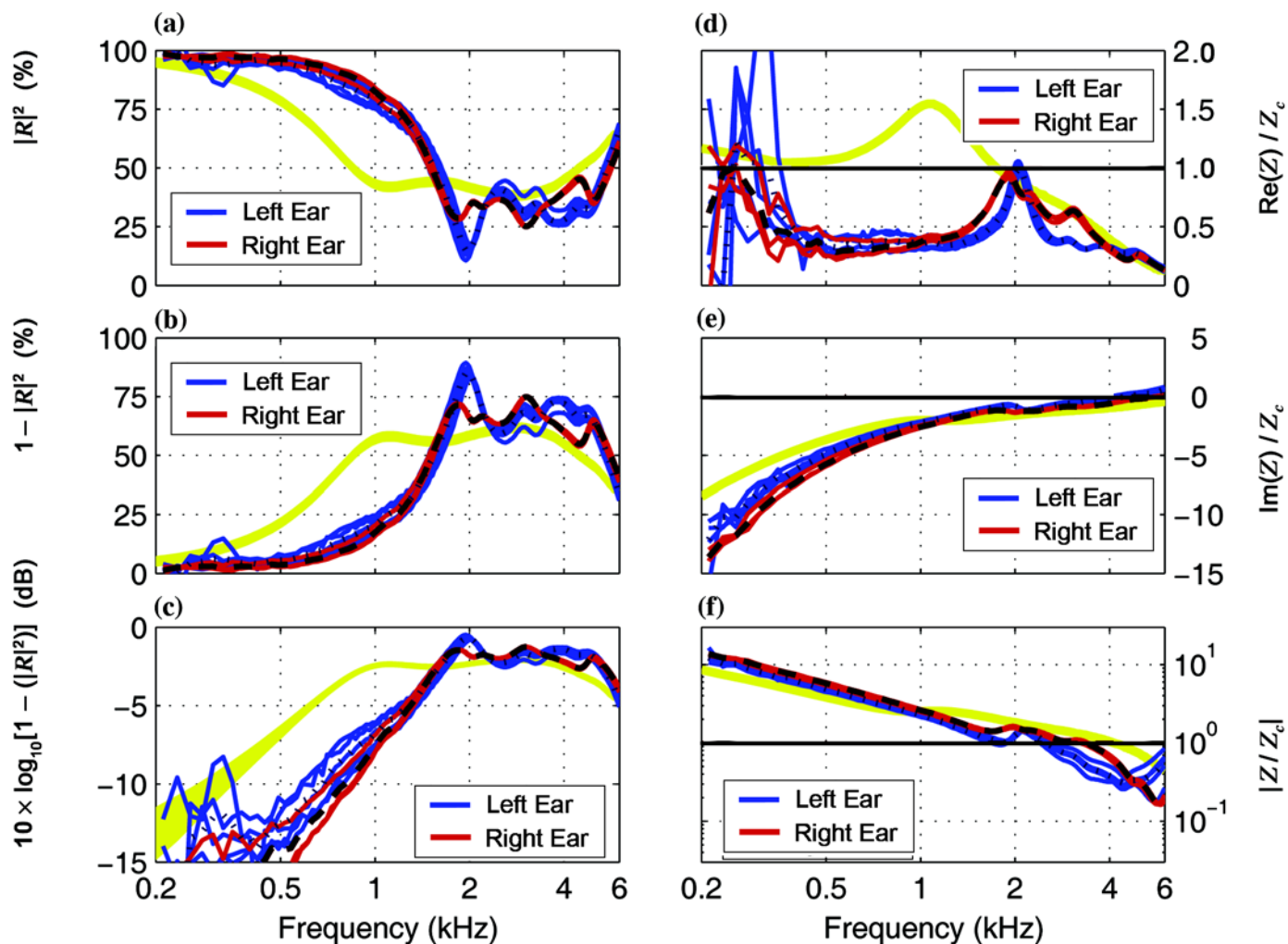


Figure 2.

Adult female with bilateral otosclerosis: Acoustic properties measured in both ears (red for right ear and blue for left) are compared with those of control (standard artificial ear coupler [yellow]) (means in black dashed lines). (a) Power reflectance ($|R|^2$) in percent, (b) power absorption ($1 - |R|^2$) in percent, and (c) transmittance ($10 \times \log_{10}[1 - (|R|^2)]$) in decibels. (d) Normalized resistance, real (Re) component [$\text{Re}(Z)/Z_c$]; (e) normalized reactance, imaginary (Im) component [$\text{Im}(Z)/Z_c$]; and (f) normalized impedance magnitude ($|Z/Z_c|$) compared with standard artificial ear coupler. Normalized values were obtained by dividing acoustic resistance, reactance, and impedance, respectively, by characteristic impedance of ear canal. Resulting normalized resistance, reactance, and impedance magnitude are dimensionless since each is ratio of two quantities with same units. Frequency ranges from 0.2 to 6.0 kHz.

reflected back into the ear canal. Between 0.4 and 2 kHz, the normalized resistance of the young adult otosclerotic ears (**Figure 2(d)**) is significantly below that of normal ME resistance. Normal ME resistance varies between 1 (at 0.4 and 2 kHz) and 1.5 (at 1 kHz). This may be explained by the earlier observation that (1) the middle ear is a low-loss transmission system and (2) the normal resistance is due to the matched cochlear load. Because of the stiff annular ligament in the otosclerotic ear, a large mismatch in impedance is seen below 2 kHz; this causes the incident

energy to be reflected back into the ear canal (**Figure 2(a)**) where it propagates unattenuated. Thus, below 2 kHz, the reflectance magnitude is close to 1 and the resistance is much smaller than normal. Below 0.4 kHz, the measurement becomes less accurate as the impedance angle approaches -90° because of the stiffness of the ear canal, which becomes relatively large in the negative direction as frequency decreases (i.e., at 0.3 kHz the stiffness is about 10 times greater than the characteristic impedance in the ear canal as shown in **Figure 2(e)**). The abnormality of

these otosclerotic ears is not as clearly evident from the impedance magnitude data (**Figure 2(f)**).

Perforated Eardrum

Figure 3 shows data for a female subject with a perforated eardrum in the right ear (solid red lines for three repeated measurements) and a normal left ear (solid blue line). The mean of the measurements for the right ear is shown by a dashed black line. The perforation in the right eardrum was a 3 to 4 mm diameter anterior, inferior, central tympanic membrane perforation; size was measured by the ear, nose, and throat doctor at the time of eardrum repair surgery. The ossicular chain was intact and subjectively mobile. The power reflectance curve (**Figure 3(a)**) for the left ear is very similar to that of a normal ear up to about 1 kHz, as represented by the standard coupler measurements. At higher frequencies, the good ear shows a lower reflectance than the standard coupler with a relatively low minimum value at 3.5 kHz, above which it becomes mass dominated, which causes the reflectance to rise rapidly above this frequency.

The ear with the perforated eardrum (right ear) shows a lower than normal power reflectance in the low-frequency region below 1.5 kHz. At higher frequencies, the power reflectance varies over a wide range, although it is consistently below that of the standard coupler. The data become erratic and it is not clear how many minima are relevant in the power reflectance curve. The power absorption data (**Figure 3(b)**) show a similar high degree of variability.

For frequencies below 1 kHz, the power flow into the ME is substantially greater than that for a normal ear (in terms of transmittance, as specified in decibels). It is not clear in this case that the absorbed power is conducted into the ME.

The transmittance curve (**Figure 3(c)**), in contrast to the power reflectance and power absorption curves, shows relatively little variability over a wide frequency range (0.4–6 kHz). Note that all three curves, power reflectance, power absorption, and transmittance, show a high degree of variability below 0.4 kHz. This variability is believed to be the result of external noise that is picked up during the measurement procedure because of the open eustachian tube of the subject.

The transmittance of the ear with the perforated eardrum is substantially higher than that of the average normal ear in the frequency region below 1 kHz, as shown by the curve for the standard coupler. In the intermediate

frequency range between 1 and 5 kHz, the transmittance is still consistently higher than that of the average normal ear but only by a small amount since the transmittance for both the normal and damaged ears is only a few decibels from the maximum transmittance of 0 dB. At frequencies above 5 kHz, the transmittance of the damaged ear remains high while that of the normal ear (i.e., standard coupler) decreases with increasing frequency.

The impedance measurements for the left ear show excellent agreement with the impedance of the standard coupler. The curves for normalized resistance, reactance, and impedance magnitude for the left ear (**Figure 3(d)–(f)**) are remarkably similar to the corresponding curves for the standard coupler over almost the entire frequency range with the only significant differences at either very high or very low frequencies. The data for the damaged ear tell a very different story. The normalized resistance (**Figure 3(d)**) differs substantially from that of a normal ear with a major peak at 2 kHz and another just above 5 kHz. The normalized reactance curve (**Figure 3(e)**) also deviates dramatically from normal below 2 kHz; this region is where stiffness-based reactance is normally dominant and the reactance of the damaged ear in this frequency region is very small and mass dominated. The resistance is also close to zero in this frequency region, and at 0.35 kHz (the frequency at which the reactance is zero), the impedance magnitude shows a sharp dip. This dip is clearly evident in **Figure 3(f)**, while the effect is not seen as easily in the normalized resistance and reactance curves.

The dip in the normalized impedance magnitude is believed to be a Helmholtz resonance effect between the ME cavity-volume stiffness and the mass of the hole in the eardrum [23–25]. At that frequency, the two reactances are equal and opposite in sign and cancel each other, which results in a sharp dip in the impedance magnitude as resistance is also close to zero in this frequency region.

Otitis Media with Effusion in a Young Child

Figure 4 shows data obtained from a 4-year-old, male child with OME. Each of the graphs consists of a solid blue line and a broad yellow region of variable width with a dotted line in the middle of the region that indicates a 30-ear mean. The solid blue line represents the data for the OME ear, while the broad yellow region with the dotted line summarizes data for 30 normal ears in the same age group (2.5 to 4 yr). The dotted line at the center of the yellow region represents the average for the 30 normal ears

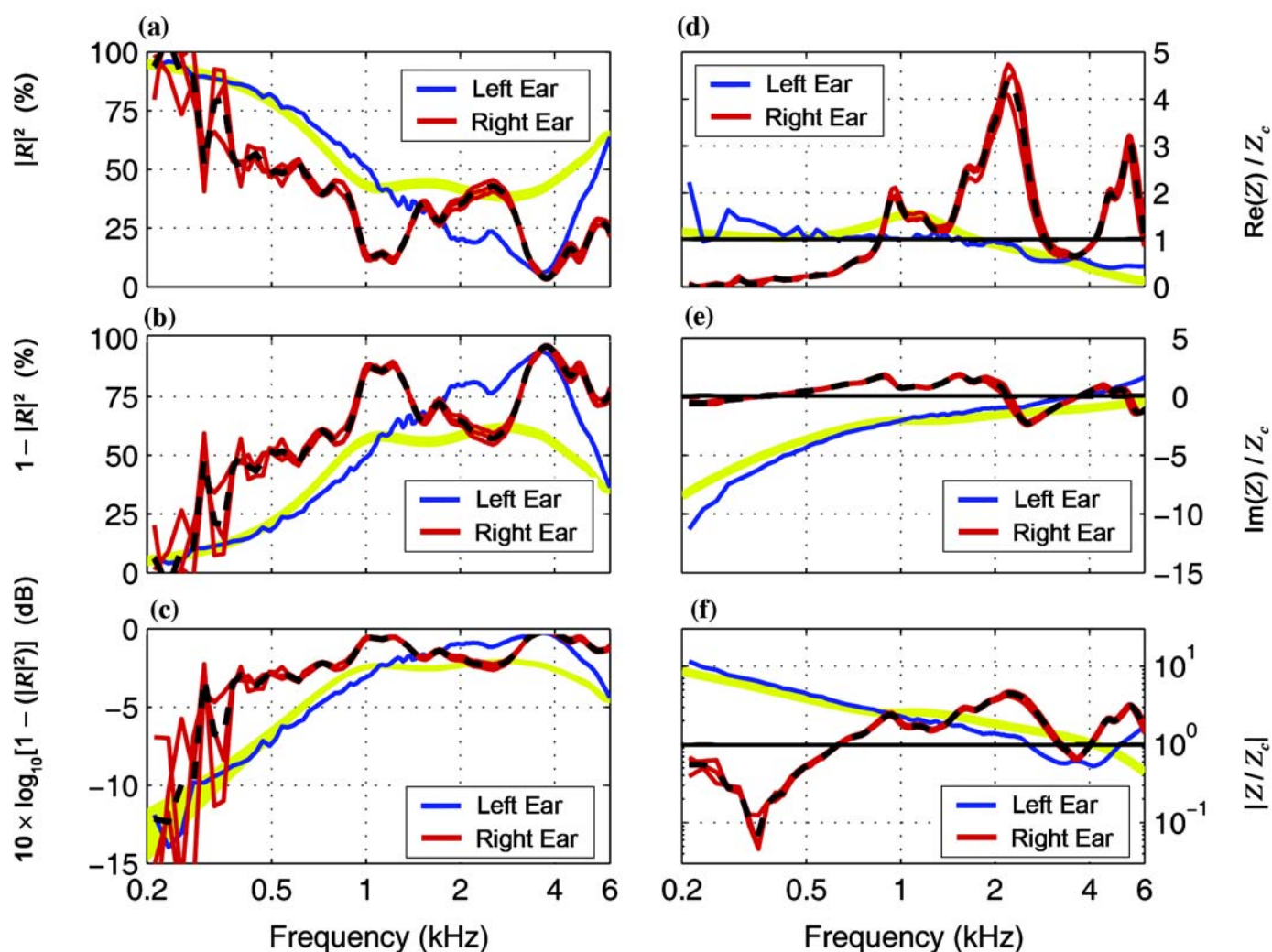


Figure 3.

Adult female with perforated eardrum: Patient has 3–4 mm diameter tympanic membrane perforation in right ear (repeated measurements in red and mean in black dashed lines) compared with relatively normal left ear (blue). Acoustic properties of two ears are compared with those of control (standard artificial ear coupler [yellow]). (a) Power reflectance ($|R|^2$) in percent, (b) power absorption ($1 - |R|^2$) in percent, and (c) transmittance ($10 \times \log_{10} [1 - (|R|^2)]$) in decibels. (d) Normalized resistance, real (Re) component [$\text{Re}(Z)/Z_c$]; (e) normalized reactance, imaginary (Im) component [$\text{Im}(Z)/Z_c$]; and (f) normalized impedance magnitude ($|Z|/Z_c$). Normalized values were obtained by dividing acoustic resistance, reactance, and impedance, respectively, by characteristic impedance of ear canal. Resulting normalized resistance, reactance, and impedance magnitude are dimensionless since each is ratio of two quantities with same units. Frequency ranges from 0.2 to 6.0 kHz.

and the boundaries represent the mean ± 1 standard deviation. These data were collected by Wei Wei Lee at Albert Einstein College of Medicine, Bronx, New York, as part of a larger study directed by Judy Gravel [21].

The power reflectance (Figure 4(a)) for the ear with OME is substantially higher than normal, which shows that at almost every frequency, most of the acoustic power that reaches the ME is reflected back into the ear canal. Similarly, power absorption (Figure 4(b)) shows

that less than half the incident power is absorbed by the ME. The transmittance for this ear (Figure 4(c)) is more than 6 dB below that of the average normal ear over the entire frequency range. Since 6 dB corresponds to a power ratio of 4:1, the transmittance indicates that less than 25 percent of the incident power is transmitted to the ME over this frequency range.

The observations are not surprising for this case since fluid in the ME restricts movement of the ossicles such

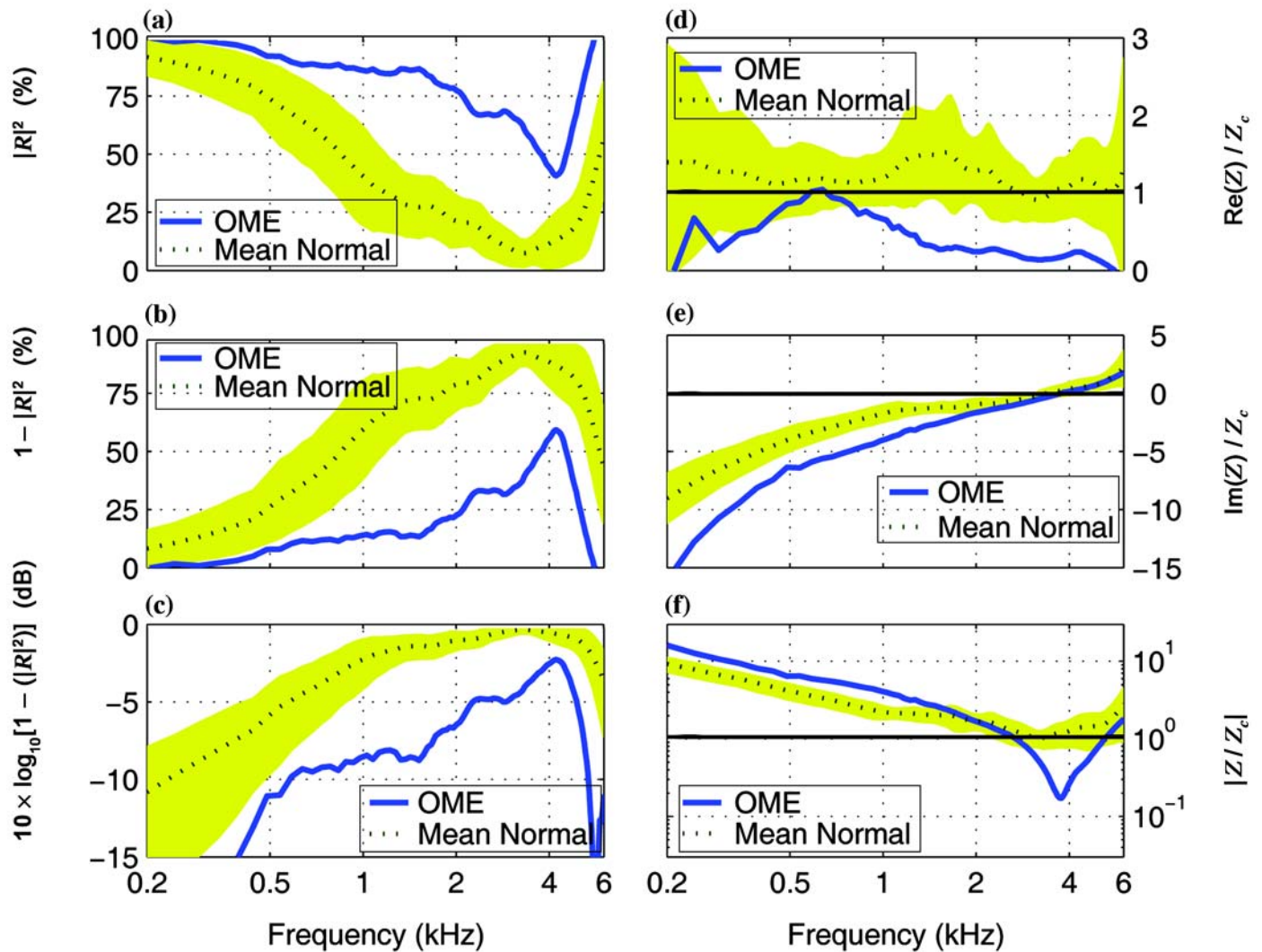


Figure 4.

Young child with otitis media with effusion (OME): This child's acoustic properties (blue) are compared with those of group of 30 young children with normal middle ear function as determined by tympanometry, otoscopic evaluation, and verbal interview. Means of normal ears are plotted as dotted lines in middle of yellow regions, which are mean ± 1 standard deviation. (a) Power reflectance ($|R|^2$) in percent, (b) power absorption ($1 - |R|^2$) in percent, and (c) transmittance ($10 \times \log_{10}[1 - (|R|^2)]$) in decibels. (d) Normalized resistance, real (Re) component [$\text{Re}(Z)/Z_c$]; (e) normalized reactance, imaginary (Im) component [$\text{Im}(Z)/Z_c$]; and (f) normalized impedance magnitude ($|Z|/Z_c$). Normalized values were obtained by dividing acoustic resistance, reactance, and impedance, respectively, by characteristic impedance of ear canal. Resulting normalized resistance, reactance, and impedance magnitude are dimensionless since each is ratio of two quantities with same units. Frequency ranges from 0.2 to 6.0 kHz.

that substantially more power is needed to move them. The reduction in transmittance is largely independent of frequency, i.e., transmittance for the ear with OME is consistently below that of the average normal ear by just over 6 dB, except in the region of 4 kHz where the difference is less than 6 dB.

The data on normalized resistance, reactance, and impedance magnitude also show consistent differences between the ear with OME and the average normal ear.

The normalized resistance (**Figure 4(d)**) is less than that of the average normal ear over the entire frequency range. While the arithmetic difference is not very large, the ratio is substantial particularly in the frequency region above 2 kHz where the normalized resistance for the OME ear is close to zero. As before, this finding is not surprising since the resistance represents that component of ME impedance that absorbs power.

The normalized reactance (**Figure 4(e)**) of the OME ear is slightly larger in magnitude than that of the average normal ear for frequencies below 2 kHz. At higher frequencies, the reactance is approximately the same as that of the normal ear. The normalized impedance magnitude (**Figure 4(f)**) shows a large difference from that of the normal ear with a marked dip just below 4 kHz.

All the OME data are significantly different from that of a normal ear. The differences, however, are larger and more noticeable in the three reflectance-based diagrams (**Figure 4(a)–(c)**). Of these, only the transmittance shows the difference between the OME ear and the average normal ear in terms of decibels, which can be related directly to other relevant audiological measures such as differences in hearing level (HL).

DISCUSSION

The data reported in this study are consistent with previous research on the use of reflectance measurements to evaluate ME function. For example, Feeney et al. found abnormal reflectance for otosclerosis (two ears), ossicular discontinuity (two ears), hypermobile tympanic membrane (two ears), perforations of the tympanic membrane (two ears), and a pressurized ME space (two ears) [22]. Hunter found significantly higher reflectance in infants and young children with OME, “poor status” ears, and cleft palates [6–7].* Others have found similar results [26].

The measurement protocol that was used in this study was developed by Allen [9] and Voss and Allen [10]. In addition to reflectance, this method also provides detailed information on related variables such as acoustic impedance. This article compared several different measurements that can be conveniently obtained with this method and that have application to the clinical assessment of ME

function. The measurements compared were a set of three reflectance-based measurements (power reflectance, power absorption, and transmittance) and a set of three normalized impedance-based measurements (acoustic resistance, acoustic reactance, and impedance magnitude). Percent power reflectance was included because of the growing interest in this property of the ear [6–9,15,25]. Percent power absorption was included since it has an obvious and useful physical interpretation. Transmittance was included because it specifies power absorption on a decibel scale and, in so doing, provides a useful link to other widely used audiological measurements such as HL. Measurements of acoustic impedance were included because of their clinical importance in the assessment of ME function. As described earlier, the impedance-based measurements (resistance, reactance, and impedance magnitude) were normalized by dividing the measured quantities by the acoustic impedance of the ear canal; this reduces between-subject variability by taking into account differences in the physical size of the ear canal and between-test variability by taking into account ambient pressure and temperature differences.

Of the reflectance-based measurements, transmittance appears to be the most useful since it is closely related to the ME transfer function and is specified in decibels. The effect of ME impairment on transmittance can be directly compared with changes in HL. The transmittance of the OME ear in **Figure 4(c)** was 6 to 10 dB below normal, which was consistent with the elevation in auditory threshold for this ear. To the best of our knowledge, no study has yet made detailed comparisons between transmittance and hearing loss.

The normal transmittance curve also has a simple shape which is useful for comparison. The transmittance of the normal ear is approximated quite well by three straight lines: an upward sloping line of 6 dB per octave at frequencies below 1 kHz, a horizontal line (slope of 0) within 3 dB of the maximum transmittance between 1 and 4 kHz, and a downward sloping line at higher frequencies (with a slope typically between –6 and 0 dB per octave); this effect is not well understood today. This overall pattern provides a convenient, well-defined reference for testing for abnormal power flow into the ME.

A problem with power reflectance measurements is their relatively high variability in the region from 1 to 3 kHz (**Figure 1(a)**) or 2 to 5 kHz (**Figure 2(a)**). These measurements can highly depend on small experimental errors when the reflectance is small. In contrast, the

*Hunter LL. Wideband reflectance of the middle ear: Implications for infant hearing assessment. The 5th Biennial Audiology Symposium. Innovations in Hearing. The Cleveland Clinic; 2004 Apr 6–7; Cleveland, OH.

Hunter LL, Jeng P, Jackson A, Propes S. Detection of otitis media with effusion using wideband reflectance in children. Proceedings of the 5th Extraordinary International Symposium on Recent Advances in Otitis Media: Innovations in Otitis Media; 2005 Apr 24–27; Amsterdam, the Netherlands.

Hunter LL. Wideband reflectance in healthy newborns and infants with cleft palate. Research Seminar at the Karolinska Institute; 2001 Sep; Stockholm, Sweden.

transmittance data showed little variability in the frequency regions where reflectance is small because the maximum transmittance was 0 dB. The small variability of transmittance data makes determining when the power flow into the ear is normal easier. The transmittance is more characteristic of hearing threshold measurements than the power reflectance. Another problem with reflectance measurements that does not apply to transmittance is the difficulty of establishing the normal curve in the frequency region of minimum reflectance. Simple averages of many curves can result in a highly biased estimate; this is not an issue with transmittance data.

Measurements of power absorption are more easily interpreted than those of power reflectance since it is the absorbed power that determines the sensitivity of the ear. Power absorption measurements, however, are relatively more variable in the region of maximum power absorption because power absorption is directly related (with no change in scale) to power reflectance.

The measurements of normalized acoustic resistance and reactance have been shown to be very useful and supplement transmittance data when ME status is being evaluated. Sharp minima in impedance magnitude indicate a special problem. At high frequencies, such minima correspond to mass dominance, which may indicate high-frequency problems, while at low frequencies may indicate an eardrum perforation. Such sharp notches are consistent with most of the energy being reflected by the ME. Notches of this magnitude are of special significance, with the frequency of the notch correlated with the type of abnormality [23–25].

CONCLUSIONS

In summary, transmittance appears to be the most useful single measure. It shows distinct differences among common ME pathologies that are easy to identify because the transmittance curves are relatively smooth. In addition, the deviation from normal transmittance may be measured in decibels, which specifies the effect of the impairment in audiological terms. The shape of the normal transmittance curve appears to approximate the ME transfer function, which allows for convenient assessment of abnormal transmittance data. Transmittance, however, does not tell the whole story, and it is advisable that it be used in conjunction with measures of resistance, reactance, and impedance magnitude.

ACKNOWLEDGMENTS

We would like to thank Dr. Michael Novak for his assistance. Mimoso Acoustics, Inc., developed the equipment used for the measurements we report in this article under a Small Business Innovation Research grant from the National Institute on Deafness and Other Communication Disorders (grant 1 R43 DC03138-01).

REFERENCES

1. Lynch TJ 3rd, Peake WT, Rosowski JJ. Measurements of the acoustic input-impedance of cat ears: 10 Hz to 20 kHz. *J Acoust Soc Am.* 1994;96(4):2184–2209.
2. Norton SJ, Gorga MP, Widen JE, Folsom RC, Sininger Y, Cone-Wesson B, Vohr BR, Fletcher KA. Identification of neonatal hearing impairment: A multi-center investigation. *Ear Hear.* 2000;21(5):348–56.
3. Gorga MP, Preissler KJ, Simmons LW, Hoover B. Some issues relevant to establishing a universal newborn hearing screening program. *J Am Acad Audiol.* 2001;12(2):101–12.
4. Orlando MS, Prieve BA. Models for universal newborn hearing screening programs. In: Spivack LG, editor. *Universal newborn hearing screening.* New York (NY): Thieme; 1998. p. 50–66.
5. White KR, Vohr BR, Behrens TR. Universal newborn hearing screening using transient evoked otoacoustic emissions: Results of the Rhode Island Hearing Assessment Project. *Semin Hear.* 1993;14:18–29.
6. Hunter LL. Wideband reflectance in infants and children with middle ear effusion [abstract]. 2004 American Auditory Society Science and Technology Meeting; 2004 Mar 7–9; Scottsdale, AZ. Dammeron Valley (UT): American Auditory Society; 2004.
7. Hunter LL, Tubaugh L, Propes S. Reliability of wideband reflectance in healthy children. American Academy of Audiology 17th Annual Convention and Expo [abstract RP406]; 2005 Mar 30–Apr 2; Washington, DC. Reston (VA): American Academy of Audiology; 2005.
8. Vander Werff KR, Prieve BA. Test-retest reliability of wide-band reflectance measures in infants. 27th Annual Midwinter Meeting of the Association for Research in Otolaryngology; 2004 Feb 22–26; Daytona Beach, FL. Mt. Royal (NJ): Association for Research in Otolaryngology; 2004. p. 777.
9. Allen JB. Measurement of eardrum acoustic impedance. In: Hall JL, Allen JB, Hubbard A, Neely ST, Tubis A, editors. *Peripheral auditory mechanisms.* New York (NY): Springer-Verlag; 1986. p. 44–51.

10. Voss SE, Allen JB. Measurement of acoustic impedance and reflectance in the human ear canal. *J Acoust Soc Am*. 1994;95(1):372–84.
11. Keefe DH. Method to measure acoustic impedance and reflection coefficient. *J Acoust Soc Am*. 1992;91(1):470–85.
12. Keefe DH, Bulen JC, Arehart KH, Burns EM. Ear-canal impedance and reflection coefficient in human infants and adults. *J Acoust Soc Am*. 1993;94(5):2617–38.
13. Lynch TJ 3rd, Nedzelnitsky V, Peake WT. Input impedance of the cochlea in cat. *J Acoust Soc Am*. 1982;72(1):108–30.
14. Puria S, Allen JB. Measurement and model of the cat middle ear: evidence of tympanic membrane acoustic delay. *J Acoust Soc Am*. 1998;104(6):3463–81.
15. Beranek LL. *Acoustic measurements*. New York (NY): John Wiley & Sons; 1949.
16. Neely S, Gorga MP. Comparison between intensity and pressure as measures of sound level in the ear canal. *J Acoust Soc Am*. 1998;104(5):2925–34.
17. Shaw E. The acoustics of the external ear. In: Studebaker GA, Hochberg I, editors. *Acoustical factors affecting hearing aid performance*. Baltimore: University Park Press; 1980. p. 109–25.
18. Margolis RH, Saly GL, Keefe DH. Wideband reflectance tympanometry in normal adults. *J Acoust Soc Am*. 1999;106(1):265–80.
19. Keefe DH, Simmons JL. Energy transmittance predicts conductive hearing loss in older children and adults. *J Acoust Soc Am*. 2003;114(6 Pt 1):3217–38.
20. Mimoso Acoustics, Inc. *CubeDis Distortion Product Otoacoustic Emission Measurement System, Version 3.0*. Mimoso Acoustics, Inc.: (IL); 1994.
21. Jeng PS, Levitt H, Lee WW, Gravel JS. Reflectance measurements for detecting OME in children: Preliminary findings. In: Bluestone CD, Casselbrant, Bakaletz, Giebink, Klein JO, Demaria, Ogra, Lim DJ, editors. *Recent Advances in Otitis Media with Effusion: Proceedings of the 7th International Symposium*; 1999 Jun 1–5; Ft. Lauderdale, FL. Hamilton, Ontario (Canada): BC Decker; 2002. p. 194–99.
22. Feeney MP, Grant IL, Marryott LP. Wideband energy reflectance measurements in adults with middle-ear disorders. *J Speech Lang Hear Res*. 2003;46(4):901–11.
23. Voss SE, Rosowski JJ, Merchant SN, Peake WT. How do tympanic-membrane perforations affect human middle-ear sound transmission *Acta Otolaryngol*. 2001;121(2):169–73.
24. Voss SE, Rosowski JJ, Merchant SN, Peake WT. Middle-ear function with tympanic-membrane perforations. I. Measurements and mechanisms. *J Acoust Soc Am*. 2001;110(3 Pt 1):1432–44.
25. Voss SE, Rosowski JJ, Merchant SN, Peake WT. Middle-ear function with tympanic-membrane perforations. II. A simple model. *J Acoust Soc Am*. 2001;110(3 Pt 1):1445–52.
26. Keefe DH, Gorga MP, Neely ST, Zhao F, Vohr B. Ear-canal acoustic admittance and reflectance measurements in human neonates. II. Predictions of middle-ear dysfunction and sensorineural hearing loss. *J Acoust Soc Am*. 2003;113(1):407–22.

Submitted for publication April 6, 2005. Accepted in revised form June 27, 2005.

